

AN *XMM-NEWTON* SEARCH FOR X-RAY EMISSION FROM THE MICROLENSING EVENT MACHO-96-BLG-5

A. A. NUCITA, F. DE PAOLIS, G. INGROSSO, AND D. ELIA

Dipartimento di Fisica, Università degli Studi di Lecce; and INFN, Sezione di Lecce, C.P. 193, I-73100 Lecce, Italy

AND

J. DE PLAA¹ AND J. S. KAASTRA

SRON Netherlands Institute for Space Research, Sorbonnelaan 2, NL-3584 CA Utrecht, Netherlands

Received 2006 April 14; accepted 2006 July 14

ABSTRACT

MACHO-96-BLG-5 was a microlensing event observed toward the bulge of the Galaxy with an exceptionally long duration of ~ 970 days. The microlensing parallax fit parameters were used to estimate a lens mass $M = 6_{-3}^{+10} M_{\odot}$, corresponding to a distance d in the range 0.5–2 kpc. The upper limit on the absolute brightness for main-sequence stars of the same mass is less than $1 L_{\odot}$, so the lens is a good black hole candidate. Such a black hole would accrete from the interstellar medium, thereby emitting in the X-ray band. Here we report the analysis of a deep *XMM-Newton* observation toward the MACHO-96-BLG-5 lens position. Only an upper limit (99.8% confidence level) to the X-ray flux from the lens position, 9.10×10^{-15} to 1.45×10^{-14} ergs cm⁻² s⁻¹ in the 0.2–10 keV energy band, is obtained, allowing us to constrain the putative black hole’s accretion parameters.

Subject headings: black hole physics — stars: individual (MACHO-96-BLG-5) — X-rays: stars

1. INTRODUCTION

Gravitational microlensing (Paczynski 1986, 1996) is nowadays a well-established technique to map both visible and dark matter throughout the Galaxy. The first lines of sight to be explored were those toward the Magellanic Clouds and the bulge of the Galaxy, leading to the observation of several hundred microlensing events (Alcock et al. 2000b; Sumi et al. 2006). The interpretation of the observations, although debated and controversial, supports the existence in the Galactic halo of MACHOs (massive astrophysical compact halo objects), with masses of $\simeq 0.4 M_{\odot}$. Microlensing events toward the bulge of the Galaxy are interpreted as being due to lenses predominantly belonging to known stellar populations. However, several long-duration events toward the bulge have significant probabilities of being due to black hole (BH) lenses (Bennett et al. 2002; Mao et al. 2002).

It is well known that the light curve of a typical microlensing event depends on four parameters (e.g., the mass M of the lens, the observer-lens distance d , the observer-source distance s , and the lens transverse velocity v_{\perp}), while only two quantities are available from observations (the amplification at maximum and the event duration). Therefore, a degeneracy remains in the microlensing parameters, so that the lens mass cannot be unequivocally determined; only statistical information can be obtained, with the analysis of a large enough number of microlensing events.

The parameter degeneracy may be solved with a few parallax events, which are events with duration long enough to make it possible to estimate d , v_{\perp} , or both. In this case, fitting to the event light curve allows one to extract the value of the lens mass. This was the case for at least 22 microlensing parallax events (Poindexter et al. 2005) observed by the MACHO Collaboration toward the bulge of the Galaxy. Among these, three are particularly interesting: MACHO-96-BLG-5, MACHO-98-BLG-6, and MACHO-99-BLG-22. For these three events, the lens masses have been

estimated to be $6_{-3}^{+10} M_{\odot}$, $6_{-3}^{+7} M_{\odot}$ (Bennett et al. 2002), and $11_{-6}^{+12} M_{\odot}$ (Mao et al. 2002; Agol et al. 2002), respectively.

The observed upper limit on the absolute brightness of these lenses is $1 L_{\odot}$, so the lenses cannot be stars and are most likely black holes² (see Bennett et al. 2002). Stellar-mass BHs exist in the Galaxy as a consequence of the evolution of massive stars, but all candidates known to date are members of binary systems. On the other hand, because of the shapes of these microlensing light curves, we expect the lenses to be isolated objects, so that the coordinates of these events give us a direction in which to point an X-ray instrument to acquire information on the nature of the lens.

Indeed, a putative BH lens may be accreting interstellar gas and could be luminous in the X-ray band if it is within the thin gas layer of the Galactic disk (Mao et al. 2002). A first estimate of the X-ray flux expected in the 1–10 keV band leads to values of $\simeq 10^{-15}$ ergs cm⁻² s⁻¹ (Agol & Kamionkowski 2002).

In this paper, we report on a 100 ks *XMM* observation toward the position of MACHO-96-BLG-5 to search for an X-ray signature from the accretion processes of the BH candidate. The paper is structured as follows: In § 2, we give a short description of the event, and in § 3 we discuss the X-ray observations performed toward this target by other telescopes. In § 4, we report our observational results. Finally, in § 5 we address some conclusions.

Before closing this section, we would like to mention that detecting isolated BHs is of great importance in astrophysics, since this should allow the validation or invalidation of the standard model for stellar evolution and BH formation.³ Simple estimates indicate, in fact, that about 10^8 BHs should be present throughout the Galaxy (see, e.g., Shapiro & Teukolsky 1983), and this is in agreement with predictions from chemical enrichment by

² Poindexter et al. (2005) also concluded that MACHO-99-BLG-22 is a strong BH candidate (78%), MACHO-96-BLG-5 is a marginal candidate (37%), and MACHO-98-BLG-6 is a weak candidate (2.2%).

³ Indeed, it could be that nature has more difficulty in producing BHs than expected within the standard stellar evolution model, as has recently emerged from *Chandra* observations of the X-ray pulsar CXO J164710.2–455216 indicating that its progenitor had a mass greater than about $40 M_{\odot}$ (Muno et al. 2006).

¹ Also Sterrekundig Instituut, Universiteit Utrecht, Postbus 80000, NL-3508 TA Utrecht, Netherlands.

TABLE 1
MACHO-96-BLG-5 PARAMETERS

Parameter	Value
R.A. (J2000)	18 ^h 05 ^m 02 ^s .5
Decl. (J2000).....	-27° 42' 17"
Duration ΔT	970 \pm 20 days
Projected velocity v_{\perp}	30.9 \pm 1.3 km s ⁻¹
Mass M	6 $^{+10}_{-3}$ M_{\odot}

NOTE.—From Bennett et al. (2002).

supernovae, which indicate that about 2×10^8 BHs should have formed (Samland 1998). The MACHO and OGLE groups have claimed detection of three isolated BHs by gravitational microlensing, indicating that at most $\simeq 5 \times 10^8$ ($9 M_{\odot}/M_{\text{BH}}$) BHs reside in the Milky Way disk (Agol et al. 2002; Alcock et al. 2000a). However, the number of isolated BHs present in the Galaxy should be confirmed by direct observations of their X-ray or radio emission (Maccarone 2005).

2. THE GRAVITATIONAL LENSING EVENT MACHO-96-BLG-5

Gravitational microlensing (i.e., gravitational deflection and amplification) of electromagnetic waves is a well-known phenomenon predicted by the general theory of relativity. In the presence of a massive object (such as a MACHO, star, or stellar-mass BH) close enough to the line of sight to a star (source), an amplification of the received flux may be observed depending on the Einstein radius $R_E = [4GMd(s-d)/(c^2s)]^{1/2}$, d and s being the lens and source distances, respectively. Because of the relative transverse velocity v_{\perp} between the lens and the line of sight to the source, the amplification is time-dependent, with the duration of a microlensing event being given by $\Delta T = 2R_E/v_{\perp}$.

For most observed microlensing events, the lens mass can only be estimated very roughly based upon the observed time ΔT . In fact, since s is usually known and only two observed quantities (the maximum amplification and ΔT) are available from observations, there remains a degeneracy in the microlensing parameters.

For long enough events, it is often possible to measure parallax effects, which makes it possible to estimate the lens distance, its transverse velocity v_{\perp} , or both. In this case, a fit to the event's light curve allows one to extract the value of the lens mass. For these events, measurement of the projected speed of the lens allows one to relate the lens mass and the source distance as

$$M \simeq \frac{v_{\perp}^2 \Delta T^2 c^2}{16G} \frac{1-d/s}{d}, \quad (1)$$

from which it is possible to infer the lens mass once d is known.

Here we focus on the event MACHO-96-BLG-5, the parameters of which are given in Table 1 (from Bennett et al. 2002). This was a particularly long-duration microlensing event, so that parallax measurements were performed, allowing determination of the mass M of the lens as a function of the distance d . In Figure 1, we plot the mass M as given by equation (1) using the best-fit parameters given in Table 1. The region between the two dotted vertical lines indicates the lens mass best estimate $M = 6^{+10}_{-3} M_{\odot}$, corresponding to distances between ~ 0.5 and ~ 2 kpc.

3. PREVIOUS X-RAY OBSERVATIONS

An isolated BH may accrete the surrounding interstellar material as a consequence of its deep gravitational potential. It is thus

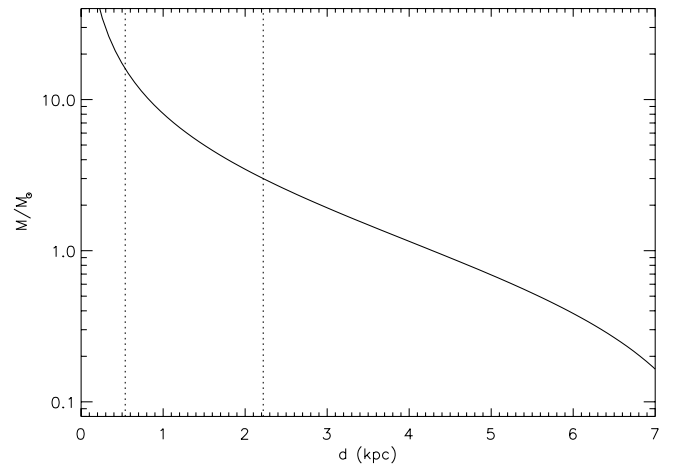


FIG. 1.—Correlation of the lens mass M with its distance d from the observer, from parallax measurements. According to the best-fit parameters given in Table 1, the most plausible lens mass value is $M = 6^{+10}_{-3} M_{\odot}$, corresponding to distances between ~ 0.5 and ~ 2 kpc (dotted vertical lines).

expected that X-ray emission, although weak (with respect to neutron stars of the same mass), should be present. This has motivated us to search for an X-ray signature from the BH candidate in the direction of MACHO-96-BLG-5.

If the BH is moving with velocity v with respect to the interstellar medium, it is expected to accrete at the Bondi-Hoyle rate, given by

$$\dot{M} = 4\pi\lambda \frac{(GM)^2}{(a_{\infty}^2 + v^2)^{3/2}} \rho_{\infty} \quad (2)$$

(Shapiro & Teukolsky 1983; see also Chisholm et al. 2003 for a more recent discussion), where λ is a constant of order unity, a_{∞} is the speed of sound in the considered medium (which is in the range 0.1–10 km s⁻¹), and ρ_{∞} is the density of the interstellar medium. Thus, the X-ray flux at Earth is

$$F_X = F_s \left(\frac{M}{1 M_{\odot}} \right)^2 \left(\frac{1 \text{ kpc}}{d} \right)^2, \quad (3)$$

where F_s is a scale flux, defined as

$$F_s = G^2 c^2 \frac{\epsilon \rho_{\infty}}{(a_{\infty}^2 + v^2)^{3/2}} \left(\frac{1 M_{\odot}}{1 \text{ kpc}} \right)^2. \quad (4)$$

Assuming $\rho_{\infty} \simeq 8.35 \times 10^{-25}$ g cm⁻³ (corresponding to $n \simeq 0.5$ cm⁻³, as expected for interstellar matter), $\epsilon = 0.1$, and $v \simeq 30$ km s⁻¹ (as given by the microlensing event observation), we have $F_s \simeq 4.45 \times 10^{-15}$ ergs cm⁻² s⁻¹.

Two observations have been carried out previously toward MACHO-96-BLG-5, by the *ROSAT* and *Chandra* satellites. Maeda et al. (2005) have determined that a 9.7 ks *ROSAT* observation in the 0.1–2.4 keV band (Voges et al. 1999) permitted detection of 93 photons from a circular source region of radius 74" and of 108 photons from an annular background region with inner and outer radii of 74" and 120". Since the expected background counts work out to be $\simeq 0.00385$ arcsec⁻², the number of background counts in the source circle is $\simeq 66$. This corresponds to a source count number as high as $\simeq 27$, corresponding to a signal-to-noise ratio of $27/\sqrt{93} \simeq 2.8$. This signal-to-noise ratio is marginally

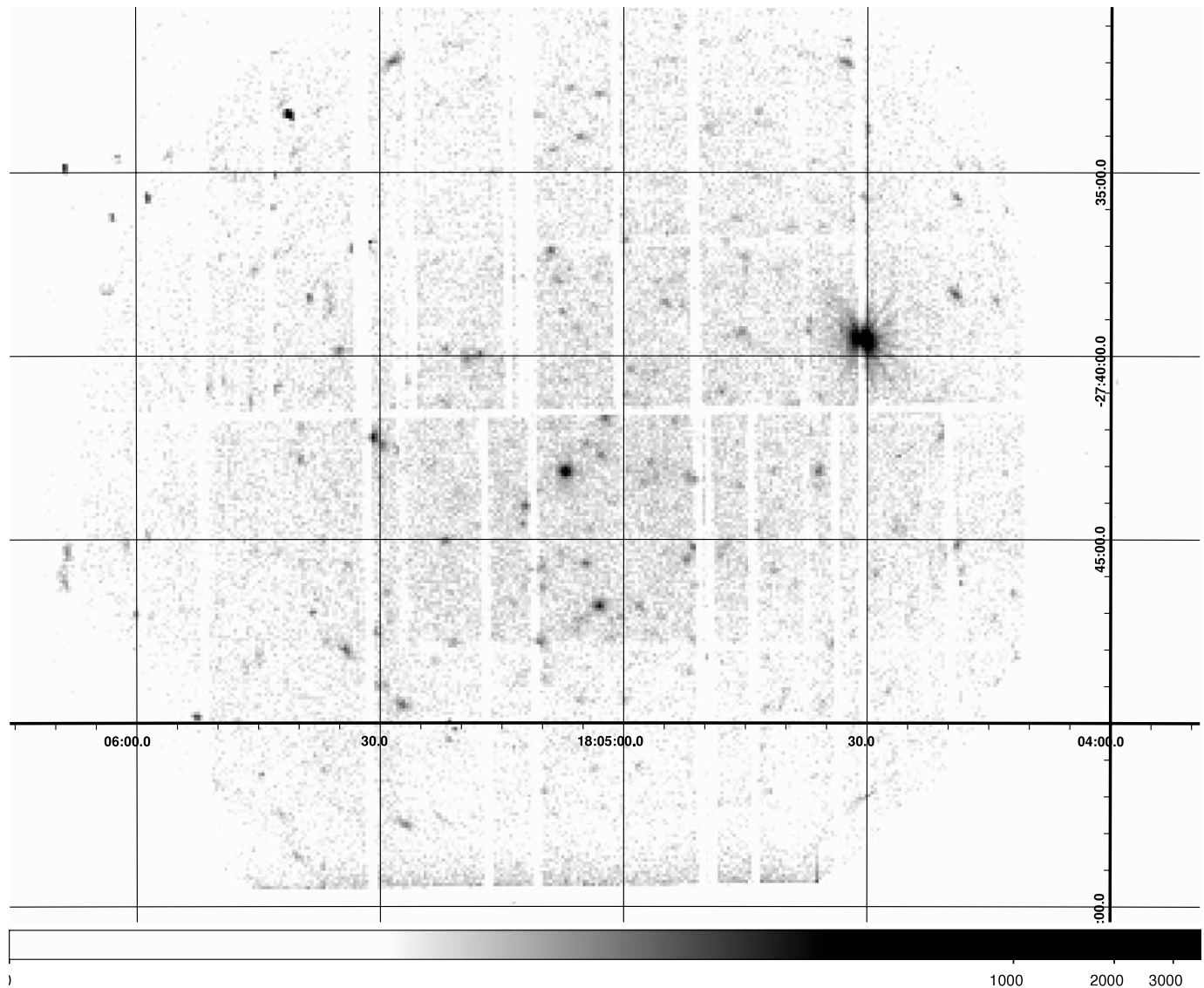


Fig. 2.—The deep *XMM* exposure, showing the existence of a number of new X-ray sources (which will be investigated elsewhere).

consistent with a source detection with a 2.8σ excess with flux of $\sim 4 \times 10^{-14}$ ergs cm^{-2} s^{-1} in the 0.1–2.4 keV band, or $\sim 1 \times 10^{-13}$ ergs cm^{-2} s^{-1} at 0.3–8 keV, where a photon index of 2 and an absorbing column density of 3×10^{21} cm^{-2} have been assumed (Maeda et al. 2005).

The X-ray signature from MACHO-96-BLG-5 has also been searched for with a 10 ks *Chandra* observation (Maeda et al. 2005). In this case, the *Chandra* ACIS-S image in the 0.3–8 keV band shows that not even a single photon was detected within $1''$ of the target position. In addition, $\simeq 21$ counts were detected within a circular region of $30''$ radius centered on the MACHO-96-BLG-5 source. Hence, the background counts around the target are $\simeq 7 \times 10^{-3}$ arcsec $^{-2}$, which is consistent with the non-detection of source photons within $1''$ from MACHO-96-BLG-5's position. Using a simple Poissonian distribution, Maeda et al. (2005) found an upper limit of 4.6 counts at 99% confidence and suggested that deeper observations ($\gg 10$ ks) with *Chandra* or *XMM-Newton* could detect, in principle, the weak X-ray signature from the lens of MACHO-96-BLG-5 if it really is a BH. Assuming an interstellar column density of $\simeq 3 \times 10^{21}$ cm^{-2} , Maeda et al. found that the previous count estimate corresponds

to fluxes of 5×10^{-15} and 4×10^{-15} ergs cm^{-2} s^{-1} for photon indices of 1.4 and 2, respectively.

4. *XMM* OBSERVATION AND RESULTS

A 100 ks *XMM* observation toward the coordinates of MACHO-96-BLG-5 was made in 2005 October (ObsID 30597) with both MOS and pn cameras operating with the thin filter in full-frame mode. The EPIC Observation Data Files were processed using the *XMM-Newton* Science Analysis System (SAS ver. 6.5.0). With the latest calibration constituent files available in 2006 May, we have processed the raw data with the *emchain* and *epchain* tools to generate proper event list files. We then only considered events with patterns 0–12 and 0–4, respectively, for the MOS and pn instruments, and we applied the respective filtering criteria *XMMEA_EM* and *FLAG* = 0, as recommended by Science Operations Centre technical note XMM-SOC-PS-TN-43, version 3.0. We used the *evselect* tool to extract light curves and images from the data. For our pointing, we rejected time periods affected by soft proton flares, which are evident in the extracted light curves as spikes. For this purpose, we built light curves for the MOS and pn instruments at energies above 10 keV (in

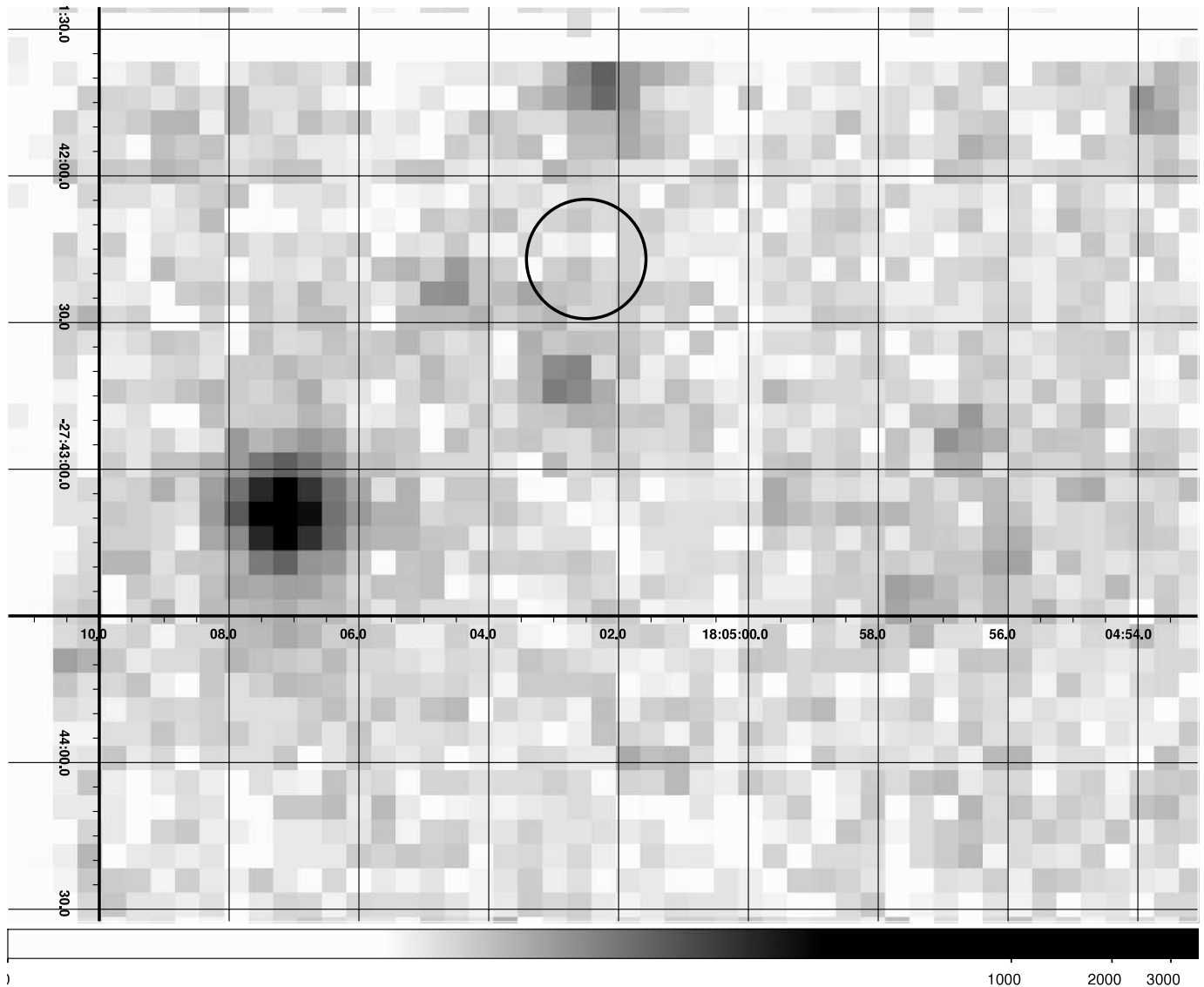


FIG. 3.—Enlargement of the *XMM* exposure around the coordinates of the MACHO-96-BLG-5 target. In particular, the circle with radius $\simeq 15''$ (each pixel is $\simeq 5''$) is centered on the target coordinates given in Table 1.

particular, in the 10–12 keV energy band), where the effect of soft proton flares is more evident. These data were recursively cleaned by removing all bins with counts more than 3σ above the mean. A new mean and new deviation were then found, and the entire process was repeated until a mean count rate per bin was reached. This procedure, when applied to the MOS and pn data, allowed us to discard high-background observing periods on the basis of the derived thresholds of 22.5 counts (or $0.225 \text{ counts s}^{-1}$) for MOS1, 26.0 counts (or $0.26 \text{ counts s}^{-1}$) for MOS2, and 49.04 counts (or $0.490 \text{ counts s}^{-1}$) for pn. Hence, with the `tabgtigen` tool, good time intervals (GTIs) were obtained and used to produce adequate X-ray event lists for each instrument. The remaining GTIs added up to result in effective exposures of $\simeq 95$, $\simeq 98$, and $\simeq 67$ ks for MOS1, MOS2, and pn, respectively.

In Figure 2, we show the full *XMM* field of view (as a composite image of the MOS1, MOS2, and pn images in the 0.2–10 keV band) toward the MACHO-96-BLG-5 region. This deep exposure reveals the existence of several new X-ray sources (not seen in previous X-ray observations), which will be investigated elsewhere. In Figure 3, we show an enlargement of the previous

figure around the coordinates of the MACHO-96-BLG-5 target. In particular, the circle with radius $\simeq 15''$ (each pixel is $\simeq 5''$) is centered on the target coordinates given in Table 1. As is evident from Figure 3, if an X-ray source exists in the encircled region, it must be extremely weak. In the following, we quantify this conclusion.

In order to confirm the absolute astrometry of our observations, we searched for counterparts of the putative X-ray sources in the Tycho-2 optical astrometric catalog (Høg et al. 2000), and we have found a number of objects (whose coordinates are given in Table 2) corresponding to X-ray sources present in the *XMM* field of view.

MOS1, MOS2, and pn images were produced in the 0.2–10 keV band with a binning that resulted in pixels of $5''$, close to the full width at half-maximum of the point-spread function of the EPIC instruments. None of the images showed an apparent excess in photons at the location of the source. Images in narrower energy bands across the 0.2–10 keV range (i.e., 0.2–0.5, 0.5–2, 2–4.5, 4.5–7, and 7–10 keV) were also produced, but they did not show an obvious source detection either.

TABLE 2
TYCHO-2 OPTICAL SOURCES WITH COORDINATES CORRESPONDING
TO X-RAY SOURCES IN OUR IMAGE

Source ID	R.A. (J2000)	Decl. (J2000)	V (mag)
1.....	18 05 30.75	-27 42 12.790	11.460
2.....	18 05 21.61	-27 29 40.50	11.163
3.....	18 05 40.08	-27 53 38.20	10.160
4.....	18 04 41.95	-27 30 35.60	12.141
5.....	18 05 03.55	-27 33 30.61	10.925
6.....	18 05 31.94	-27 54 36.17	11.244

NOTE.—Units of right ascension are hours, minutes, and seconds, and units of declination are degrees, arcminutes, and arcseconds.

We may also exclude the possibility that, as a consequence of proper motion, the BH candidate has moved away from its original position. This can be easily ruled out, since for a lens distance in the range 0.5–2 kpc (see Fig. 1), as deduced from the parallax measurements of MACHO-96-BLG-5, and for a conservative relative velocity between the lens and the observer of $\simeq 30 \text{ km s}^{-1}$, the lens would have moved from its original position by at most $\simeq 0''.015\text{--}0''.12$ over a period of 10 years. Hence, given the *XMM* pixel size quoted above, such motion is completely negligible in our case.

Next, we ran `edetect_chain` simultaneously on the three images (MOS1, MOS2, and pn in the 0.2–10 keV band). The subtask `eboxdetect` was used with a detection threshold of `likemin = 8` to provide a complete source list as input for subsequent tasks. No source was detected at the position of MACHO-96-BLG-5. As suggested by the User's Guide to the *XMM-Newton* Science Analysis System (Loiseau 2004),⁴ especially for cases in which an expected X-ray source is not detected by the usual source detection tasks, we used the `esenmap` command to generate a sensitivity map roughly giving point-source detection upper limits (in units of counts per second). Performing this task on the MOS1, MOS2, and pn images in the 0.2–10 keV band, we obtained rates of 3.1×10^{-4} , 3.0×10^{-4} , and 6.2×10^{-4} counts s^{-1} , respectively.⁵

The X-ray rate from MACHO-96-BLG-5 in the 0.2–10 keV band can be determined in the following alternative way: We consider a source extraction region around the target coordinates and several background extraction regions sufficiently far from any bright point source, but on the same chip where our target is supposed to be. Let us assume that the source and background extraction regions are circular with radii R_s and R_b and cover areas of A_s and A_b , respectively. For the source extraction region, we fix $R_s = 2.45$ pixels (or equivalently $12''.5$), so that at least 65% (respectively, 60%) of the encircled energy is collected when the MOS (pn) instrument is used. In the case of the background extraction region, a radius $R_b = 10$ (6) pixels is chosen for MOS1 and MOS2 (pn). Therefore, the covering areas are $A_s \simeq 475 \text{ arcsec}^2$ and $A_b \simeq 7775 \text{ arcsec}^2$ for MOS1 and MOS2, and $A_b \simeq 2735 \text{ arcsec}^2$ for pn. We also emphasize that the source extraction region has been chosen to be smaller than the background extraction region to avoid strong contamination by nearby sources.

⁴ See http://xmm.esac.esa.int/external/xmm_user_support/documentation/sas_usg/USG.

⁵ For comparison, the weakest source detected with the automatic procedure has a cumulative count rate of 1.7×10^{-3} counts s^{-1} (2.2×10^{-4} for MOS1, 5.4×10^{-4} for MOS2, and 9.3×10^{-4} for pn).

Let N_{s+b} and N_b be the number of counts expected within the source and background regions, respectively. We assume that within the source circle, the observed number of counts depends on the properties of both the source and the background, while the counts eventually observed within the background region are due to background only. In this case, the number of counts due to the source is

$$N_s = N_{s+b} - \frac{A_s}{A_b} N_b. \quad (5)$$

We tested different choices of background region positions until we were satisfied that the contamination due to close sources was properly subtracted. The number of counts detected within the circle (with radius R_s) centered on the nominal source position was 60, 73, and 252 in the MOS1, MOS2, and pn cameras, respectively. Using the tables given by Gehrels (1986), this leads to single-sided 3σ (or 99.8%) upper limits of 87.1, 102.5, and 303.4 on the total counts. The expected background counts (after correcting for exposure map differences and re-scaling for the extraction area) are 56, 64, and 227 for MOS1, MOS2, and pn, respectively. Correcting for the background, one has 31.1, 38.5, and 76.4 counts, corresponding to rates of 3.2×10^{-4} , 3.9×10^{-4} , and 1.0×10^{-3} counts s^{-1} , respectively.

We have also evaluated the expected 0.2–10 keV flux upper limit using PIMMS (the Portable, Interactive Multi-Mission Simulator). For this purpose, we assumed an interstellar absorption column density of $3.81 \times 10^{21} \text{ cm}^{-2}$ (as estimated by the nH HEASARC tool) and a power-law spectrum with indices Γ of 1.5 and 2.5. For the MOS1 instrument, the previously quoted count rates correspond to unabsorbed fluxes of 9.10×10^{-15} ergs $\text{cm}^{-2} \text{ s}^{-1}$ ($\Gamma = 1.5$) and 1.20×10^{-14} ergs $\text{cm}^{-2} \text{ s}^{-1}$ ($\Gamma = 2.5$). For MOS2, we obtain unabsorbed fluxes of 1.12×10^{-14} ergs $\text{cm}^{-2} \text{ s}^{-1}$ ($\Gamma = 1.5$) and 1.45×10^{-14} ergs $\text{cm}^{-2} \text{ s}^{-1}$ ($\Gamma = 2.5$). For EPIC-pn, we find 1.03×10^{-14} ergs $\text{cm}^{-2} \text{ s}^{-1}$ ($\Gamma = 1.5$) and 1.28×10^{-14} ergs $\text{cm}^{-2} \text{ s}^{-1}$ ($\Gamma = 2.5$). Therefore, we can set an upper limit on the flux from the putative source in the range 9.10×10^{-15} to 1.45×10^{-14} ergs $\text{cm}^{-2} \text{ s}^{-1}$.

5. DISCUSSION AND CONCLUSIONS

MACHO-96-BLG-5 was a microlensing observed event toward the bulge of the Galaxy with an exceptionally long duration of ~ 970 days.⁶ Measurement of the parallax angle (Bennett et al. 2002) made it possible to estimate both the lens mass ($M = 6_{-3}^{+10} M_\odot$) and its distance from Earth ($d = 0.5\text{--}2$ kpc).

Since the observed upper limit on the absolute brightness of main-sequence stars for this lens is $1 L_\odot$, MACHO-96-BLG-5 is a BH candidate. Such a BH would accrete from the interstellar medium (by means of the Bondi-Hoyle mechanism), thereby emitting X-rays. Here we have reported on a deep *XMM* observation in the 0.2–10 keV band toward the MACHO-96-BLG-5 lens position. The analysis of the observations (see § 4) did not show any obvious source and is consistent with a non-detection of the source. However, it is possible to estimate an upper limit on the source luminosity, which turns out to be in the range 9.10×10^{-15} to 1.45×10^{-14} ergs $\text{cm}^{-2} \text{ s}^{-1}$ depending on the power-law index Γ .

This upper limit allows us to constrain the accretion parameters of the candidate BH from a parametric study involving

⁶ We also note that Poindexter et al. (2005) presented best-fit solutions for the geocentric timescale of the same microlensing event and found that the event duration was 546 ± 165 days or 698 ± 303 days. This leads to the conclusion that the lens of MACHO-96-BLG-5 is a BH with a probability of about 37%.

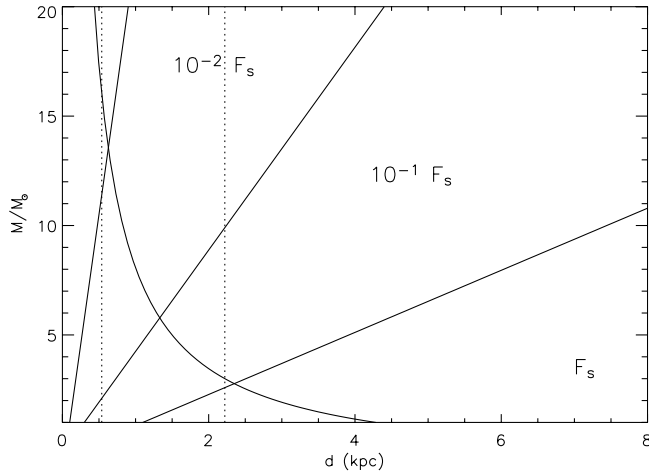


FIG. 4.—Regions (below each diagonal line) in the mass-distance plane (cf. Fig. 1) where the X-ray flux due to Bondi accretion is below the upper limit flux of 9.10×10^{-15} ergs cm^{-2} s^{-1} .

equations (3) and (4). In the BH mass-distance plane shown in Figure 4, the curved line corresponds to the mass-distance relation (also given in Fig. 1). Our candidate BH should lie on this curve (if its transverse velocity is $\simeq 30$ km s^{-1}) and within the two dotted vertical lines. The three diagonal lines correspond to the X-ray upper limit of 9.10×10^{-15} ergs cm^{-2} s^{-1} for three different values of the scale flux (F_s , $10^{-1}F_s$, and $10^{-2}F_s$). Obviously, varying F_s implies that the accretion parameters (ϵ , ρ_∞ , and v) are changing. Thus, the region below the line labeled F_s corresponds to $F_X < 9.10 \times 10^{-15}$ ergs cm^{-2} s^{-1} . The same

holds for the regions below the other two lines. It is worth noting that a BH accreting with $\rho_\infty \simeq 8.35 \times 10^{-25}$ g cm^{-3} , $\epsilon = 0.1$, and $v \simeq 30$ km s^{-1} (implying $F_s \simeq 4.45 \times 10^{-15}$ ergs cm^{-2} s^{-1}) is inconsistent with the best-fit values (mass and distance) for the MACHO-96-BLG-5 lens candidate. However, for less efficient Bondi accretion ($\epsilon \simeq 10^{-5}$ to 10^{-3}) the regions below the other two diagonal lines show that agreement is recovered.

Finally, it could be interesting to estimate the BH radiative efficiency $\eta = L_X/L_{\text{Edd}}$ with respect to the maximum allowed BH accretion rate given by the Eddington luminosity, $L_{\text{Edd}} \simeq 1.38 \times 10^{38} M / (1 M_\odot)$ ergs s^{-1} . By using the BH mass and distance ranges, namely, $3 M_\odot < M < 16 M_\odot$ and $0.5 \text{ kpc} < d < 2 \text{ kpc}$, we can compare the Eddington luminosity with the X-ray luminosity, given by $L_X = F_X 4\pi d^2$, expected for MACHO-96-BLG-5. This procedure gives η in the range 1.2×10^{-10} to 2.7×10^{-9} , in agreement with the efficiency estimates for BH accretion in quiescent galaxies and ultra-low-luminosity active galactic nuclei, for which $\eta = 4 \times 10^{-12}$ to 6×10^{-7} (Baganoff et al. 2003).

This work has been partially supported by the Italian Ministero dell'Università e della Ricerca through PRIN 2004 (No. 2004020323004). A. A. N. is grateful to SRON for the research facilities and the kind hospitality. We are also grateful to A. F. Zakharov and B. M. T. Maiolo for interesting discussions. The authors would like to thank the anonymous referee for suggestions that improved the manuscript. *XMM-Newton* is an ESA science mission with instruments and contributions funded by ESA member states and NASA.

REFERENCES

- Agol, E., & Kamionkowski, M. 2002, MNRAS, 334, 553
 Agol, E., Kamionkowski, M., Koopmans, L. V. E., & Blandford, R. D. 2002, ApJ, 576, L131
 Alcock, C., et al. 2000a, ApJ, 541, 734 (erratum 557, 1035 [2001])
 ———. 2000b, ApJ, 542, 281
 Baganoff, F. K., et al. 2003, ApJ, 591, 891
 Bennett, D. P., et al. 2002, ApJ, 579, 639
 Chisholm, J. R., Dodelson, S., & Kolb, E. W. 2003, ApJ, 596, 437
 Gehrels, N. 1986, ApJ, 303, 336
 Høg, E., et al. 2000, A&A, 355, L27 (erratum 363, 385)
 Loiseau, N., ed. 2004, User's Guide to the *XMM-Newton* Science Analysis System (issue 3.1; Madrid: European Space Astron. Cent.)
 Maccarone, T. J. 2005, MNRAS, 360, L30
 Maeda, Y., Kubota, A., Kobayashi, Y., Itoh, A., Kunieda, H., Terashima, Y., & Tsuboi, Y. 2005, ApJ, 631, L65
 Mao, S., et al. 2002, MNRAS, 329, 349
 Munro, M. P., et al. 2006, ApJ, 636, L41
 Paczyński, B. 1986, ApJ, 304, 1
 ———. 1996, ARA&A, 34, 419
 Poindexter, S., Afonso, C., Bennet, D. P., Glicenstein, J.-F., Gould, A., Szymański, M. K., & Udalski, A. 2005, ApJ, 633, 914
 Samland, M. 1998, ApJ, 496, 155
 Shapiro, S. L., & Teukolsky, S. A. 1983, Black Holes, White Dwarfs, and Neutron Stars (New York: Wiley)
 Sumi, T., et al. 2006, ApJ, 636, 240
 Voges, W., et al. 1999, A&A, 349, 389